ARTICLE
Journal of Cellular Biochemistry 115:1196–1205 (2014)

Journal of Cellular Biochemistry

# MicroRNA-190 Regulates Hypoxic Pulmonary Vasoconstriction by Targeting a Voltage-Gated $K^+$ Channel in Arterial Smooth Muscle Cells

Shan-Shan Li,[1,2] Ya-Juan Ran,[1] Dan-Dan Zhang,[1] Shu-Zhen Li,[1] and Daling Zhu[2,3]*

[1]*Department of Biopharmaceutical Sciences, College of Pharmacy, Harbin Medical University, China*

[2]*Department of Biopharmaceutical Key Laboratory of Heilongjiang Province, 157 Baojian Road, Nangang District, Harbin, Heilongjiang 150081, PR China*

[3]*Department of Biopharmaceutical Sciences, College of Pharmacy, Harbin Medical University-Daqing, Daqing 163319, China*

## ABSTRACT

Pulmonary arterial hypertension (PAH) is associated with sustained vasoconstriction, profound structural remodeling of vasculatures and alterations in $Ca^{2+}$ homeostasis in arterial smooth muscle cells (SMCs), while the underlying mechanisms are still elusive. By regulating the expression of proteins, microRNAs (miRNAs) are known to play an important role in cell fates including differentiation, apoptosis and proliferation, and may be involved in the development of PAH. Based on our previous study, hypoxia produced a significant increase of the miR-190 level in the pulmonary artery (PA), here, we used synthetic miR-190 to mimic the increase in hypoxic conditions and showed evidence for the effects of miR-190 on pulmonary arterial vasoconstriction and $Ca^{2+}$ influx in arterial SMCs. Synthetic miR-190 remarkably enhanced the vasoconstriction responses to phenylephrine (PE) and KCl. The voltage-gated $K^+$ channel subfamily member, *Kcnq*5, mRNA was shown to be a target for miR-190. Meanwhile, miR-190 antisense oligos can partially reverse the effects of miR-190 on PASMCs and PAs. Therefore, these results suggest that miR-190 appears to be a positive regulator of $Ca^{2+}$ influx, and plays an important role in hypoxic pulmonary vascular constriction. J. Cell. Biochem. 115: 1196–1205, 2014. © 2014 Wiley Periodicals, Inc.

**KEY WORDS:** HYPOXIC PULMONARY VASCULAR CONSTRICTION; microRNA; $Ca^{2+}$ INFLUX; Kcnq5; Kv7.5

Pulmonary arterial hypertension (PAH) is a malignant disease characterized by elevated pulmonary circulation resistance and increased pulmonary arterial (PA) pressure, leading to right ventricular failure and death [Oparil et al., 2003; Sandoval Zarate, 2006]. An early pathogenic process in the development of PAH is the increase in vasomotor tone that impedes blood ejected by the right ventricle [Guazzi et al., 1989; Archer and Rich, 2000; Eddahibi et al., 2002; Chin and Rubin, 2008; Voelkel et al., 2012]. Although the mechanisms underlying PAH are still unclear, the abnormal vasoconstriction is known to involve dysfunction of $K^+$ channels, leading to depolarization and an increase in cytosolic free $Ca^{2+}$ concentration ($[Ca^{2+}]_i$). The high $[Ca^{2+}]_i$ results in contraction of PA smooth muscle cells (PASMCs), a release vasoactive substances in the endothelium, and activation of multiple intracellular signaling systems in both [Humbert et al., 2004; Mauban et al., 2005; Remillard and Yuan, 2005].

Hypoxia is a well-known triggering event of PAH, acting to increase PA tension. The hypoxia-induced PA constriction is believed to be due to a phenomenon known as sustained pulmonary vasoconstriction (PVC) in a poorly ventilated area of the lung which tends to match ventilation with perfusion by reducing blood supply to the area. As expected, the imbalance in intracellular $Ca^{2+}$ homeostasis plays a role in the development of hypoxic PVC [Sweeney and Yuan, 2000; Mauban et al., 2005; Moudgil et al., 2005; Weir et al., 2010]. During acute hypoxia, the PVC is initiated and maintained by a persistent increase in $[Ca^{2+}]_i$ in PASMCs. A decrease

Grant sponsor: National Natural Science Foundation of China; Grant number: 30370578, 31071007; Grant sponsor: Science and technique Foundation of Harbin; Grant number: 2008AA3AS097, 2006RFXXS029; Grant sponsor: National Natural Science Foundation of China; Grant number: 81100036; Grant sponsor: Science Foundation of Health Department of Heilongjiang Provence; Grant number: 2009–250.

*Correspondence to: Dr. Daling Zhu, Department of Biopharmaceutical Sciences, College of Pharmacy, Harbin Medical University-Daqing, Daqing 163319, China. E-mail: dalingz@yahoo.com

Manuscript Received: 19 September 2013; Manuscript Accepted: 16 January 2014

Accepted manuscript online in Wiley Online Library (wileyonlinelibrary.com): 20 January 2014

DOI 10.1002/jcb.24771 • © 2014 Wiley Periodicals, Inc.

in $K^+$ channel activity can lead to depolarization, and activation of voltage-dependent $Ca^{2+}$ channels (VDCCs). The opening of the VDCCs can produce excessive $Ca^{2+}$ in the cytosol of PAMSCs and abnormal PVC.

The molecular and cellular basis underlying hypoxic PVC is still unclear. Recent studies suggest that microRNAs (miRs) may be involved. The miRs are endogenous noncoding small RNAs that negatively regulate the expression of their target genes at the post-transcriptional level. Such regulation affects diverse physiological and pathological processes underlying tumorigenesis and several cardiovascular diseases [Ikeda et al., 2007; Kumar et al., 2007; Zhang et al., 2007; Ono et al., 2011]. The involvement of miRs in the pathological process of PAH has also been suggested, although the mechanisms are still unclear [Caruso et al., 2012; Grant et al., 2013].

In our previous study, we have screened the miRs in hypoxic PAH and found seven miRs to be up-regulated by hypoxia in PAs [Li et al., 2013]. One of them, miR-138, is found to play an important role in PA remodeling during hypoxia, while the function of the other miRs in PVC remains unclear. Using bioinformatic analysis, we have found that the mRNA of *Kcnq*5 (or Kv7.5), a member of the voltage-gated $K^+$ channel family, has a sequence at 3′-UTR that may be targeted by miR-190, one of the hypoxic up-regulated miRs. Such a potential miR-190 target sequence is conserved among human, rat and mouse. The Kv7 family is composed of five subtypes (Kv7.1–7.5) that are encoded by five genes (*Kcnq1–5*), and play an important role in regulating the membrane potentials of many excitable cells [Robbins, 2001; Delmas and Brown, 2005]. Blockage of the Kv7 channels can increase vascular tone in various blood vessels including portal vein, aorta, mesenteric arteries, cerebral arteries as well as pulmonary arteries. Stimulation of the Kv7 channels can cause vasodilation of pulmonary and mesenteric arteries as a result of VSMC hyperpolarization. [Yeung and Greenwood, 2005; Joshi et al., 2006; Yeung et al., 2007; Mackie et al., 2008; Zhong et al., 2010]. Additionally, the Kv7.5 channel is expressed in various blood vessels, and has an influence on vascular reactivity to vasoconstrictors, like Arg8-vasopressin (AVP) [Mackie and Byron, 2008]. Given the crucial role of Kv7.5 in VSMC in controlling arterial tensions, miR-190 is indicated to be involved in abnormal smooth muscle contractility in hypoxic PAH. Therefore, we performed these studies.

## MATERIALS AND METHODS

### REAGENTS AND INSTRUMENTS

Antibodies against Kv7.5 and β-actin were purchased from EMD Millipore (Merck, Darmstadt, Germany) and Santa Cruz Biotechnology Inc (SantaCruz, USA), respectively. Enhanced chemiluminesence (ECL) reagents were from Amersham International (Amersham, UK). All other reagents were purchased from common commercial sources. The instruments: dissecting microscope (SMZ-168, Motic); force displacement transducer (JZ100, Gaobeidian Xinhang Electrical Equipment Limited Company); signal amplifier (600 series eight-channel amplifier, Gould, Electronics); $CO_2$ incubators (Thermo Scientific,Waltham, MA 02454, USA); inverted microscope (TE200, Nikon, Japan); confocal laser scanning microscope (Fluoview-FV300, Olympus, Japan); high performance liquid chromatography (Agilent 1200, USA).

### ANIMAL USE

Animal care and use complied with the Guide for the Care and Use of Laboratory Animals (NIH Publication 85–23, revised 1996), and were approved by the Institutional Animal Care and Use Committee of Harbin Medical University (Protocol [2009]-11). Adult male Wistar rats (180–200 g) were from the Experimental Animal Center of Harbin Medical University.

### ANIMAL MODEL AND TISSUE COLLECTION

The rat models were carried out by hypoxic raising (12% $O_2$) for 9 days as previously described [Zavisca et al., 1993]. After hypoxic raising, rats were intraperitoneally anesthetized with pentobarbital sodium 50 mg/kg of body weight. Waiting for fully anesthetized, the chest was surgically open. Then the heart and lungs from the animals were removed together, and placed in the cold phosphate-buffered saline (PBS) solution. The lungs were harvested and processed for immunohistochemistry and *in situ* hybridization. The PAs were collected for cultivation, quantitative real-time reverse-transcriptase polymerase chain reaction (qRT-PCR), and Western blot assay.

### HISTOCHEMICAL STAINING

Hematoxylin and eosin (H&E) staining was performed as previous described [Li et al., 2013]. Briefly, the lung tissues were fixed with 4% paraformaldehyde. After staining with H&E, morphological changes were viewed with Nikon Eclipse microscope (TS100). The areas of the vessel within the external elastic lamina (EEL), the internal elastic lamina (IEL), and the luminal area were measured. The intimal area (IEL–luminal area) and the medial area (EEL–IEL) were calculated. Results were described as ratios of intima to media. Morphometric analysis was analyzed with image software Image Pro Plus.

### LOCALIZATION OF miRs BY *IN SITU* HYBRIDIZATION

*In situ* hybridization was performed as previous described [Li et al., 2013]. Dig-labeled probe for Rno-miR-190 was designed and synthesized by Sangon Biotech (Shanghai, China). Morphometric analysis was analyzed with image software (Image Pro Plus).

### COMPUTATIONAL PREDICTION OF miRNA TARGET

Three established miRNA target prediction algorithms including TargetScan5.1, miRbase, and miRGene prediction analysis were used to identify the candidate miRNAs that were potentially targeted at the vasoconstriction-related genes.

### PA TRANSFECTION

The distal pulmonary arteries (200- to 500-μm outer diameter) were obtained from rat models as previous described [Zhu et al., 2003]. By rubbing the luminal surface with cotton, the de-endothelialized pulmonary arteries were cut into 2–3 mm in length and cultured under normoxic conditions (21%$O_2$/5%$CO_2$/balance $N_2$) for transfection. After growth arrest, the endothelium-denuded PAs were transfected with 2 μg mixture of different groups using X-tremeGene siRNA Transfection Reagent (Roche Applied Science, Mannheim, Germany) according to the manufacturer's instructions. Subsequently, the tissue

switched to complete DMEM (10%FBS) under normoxic for another 24–48 h as previous described [Li et al., 2010].

### TENSION STUDIES

After transfection, the endothelium-denuded PAs were switched into cold Krebs solution, in which containing (in mM): 118.0 NaCl, 25.0 $NaHCO_3$, 3.6 KCl, 1.2 $MgSO_4$, 1.2 $KH_2PO_4$, 11.0 glucose, and 2.5 $CaCl_2$, pH 7.4. During the experiments, rings from different groups were mounted on a force-electricity transducer with a 0.3 g of preload in a tissue bath and equilibrated for 30 min. The tissue bath was filled with Krebs solution and perfused with 5% $CO_2$ at 37 °C. The arterial tone was measured as changes in isometric force. Only rings that showed a clear vasoconstriction response to 10 μM phenylephrine (PE) were used in the following study.

### PASMCs CULTIVATION AND TRANSFECTION

The intrapulmonary arteries were de-endothelialized and digested as previously described [Li et al., 2013]. The digested PASMCs were then cultured in complete DMEM medium supplemented with 10% FBS, 1% streptomycin, and 1% penicillin for 3–5 days in humidified incubator with 5% $CO_2$ at 37 °C. The 2–4 generations were used for further experiments. After growth arrest, PASMCs were transfected with 2 μg mixture of different groups and switched to complete DMEM (10% FBS) for another 24–48 h cultivation.

### $Ca^{2+}$ IMAGING

The PASMCs transfected with different groups were gently digested with 0.25% Trypsin (Amresco Life Science Research, Solon, USA) and collected in normal Krebs solution, bubbled with 21% $O_2$–5% $CO_2$ for $Ca^{2+}$ imaging. Cell viability was consistently greater than 98%. $[Ca^{2+}]_i$ in PASMCs was monitored using fluo-3 acetoxymethyl ester (Fluo-3 AM) and recorded by confocal laser scanning microscope (CLSM). The cells were pretreated with 5–10 μM Fluo 3-AM for 30 min at 37 °C and then washed thoroughly with normal Tyrode's solution, in which containing (in mM): 135 NaCl, 5.4 KCl, 1.8 $CaCl_2$, 1.2 $MgCl_2$, 0.33 $NaH_2PO_4$, 10 glucose, 5 HEPES, pH 7.35, cells were then transferred to a recording chamber and perfused with normoxic Tyrode's solution for 10 min. The $[Ca^{2+}]_i$ FI was excited at 488 nm and measured at 5 s intervals, while collecting emitted light at 530 nm by confocal laser scanning microscopy (Olympus, Japan). After 20 s baseline recording, cells were exposed to 120 mM KCl to trigger extracellular $Ca^{2+}$ entry and then recorded for 300 s. The contributions of Kv7 channels to the $[Ca^{2+}]_i$ in PASMCs were performed by pre-exposing to a Kv7channel blocker (10 μM linopirdine) for at least 10 min before KCl challenge. Data analysis was performed off-line using Fluoview-FV300 (Olympus, Japan) to select cell regions and FI was extracted and analyzed with Excel (Microsoft). Changes of $[Ca^{2+}]_i$ were shown according to fluorescence traces representing FI normalized to initial fluorescence intensity ($FI_0$) in separated experiments. The analyses of area under the curve (AUC) [Zheng et al., 2008; Charlton and Vauquelin, 2010; Li et al., 2010] and the peak value of $[Ca^{2+}]_i$ $FI/FI_0$ were used to represent the intracellular $Ca^{2+}$ difference between different groups.

### qRT-PCR ANALYSIS

Analysis and quantification of miR-190 expression levels using qRT-PCR were performed with high-capacity cDNA Reverse Transcription Kit and Fast SYBR® Green Master Mix (Applied Biosystems life technology, NY, USA), following the manufacturer's instructions. Primers specific for Rno-miR-190 (MI0000933) (forward: GGGTGATATGTTTGATATATTAGG; reverase: CAGTGCGTGTCGTGGAGT) and RNU6B (U6) (NR_002752) (forward: GCTTCGGCAGCACATATACTAAAAT; reverse: CGCTTCACGAATTTGCGTGTCAT), were purchased from Sangon Biotech (Shanghai, China). qRT-PCR was performed as previous described [Li et al., 2013]. Expression level of target gene mRNA was determined by qRT-PCR utilizing total RNA from PAs. U6 was used as internal control for miR-190.

### SYNTHESIS OF miRs AND ANTI-miRs

One double stranded, chemically synthetic and optimized nucleic acids (miR-190, sense: UGAUAUGUUUGAUAUAUUAGGU; antisense: CUAAUAUAUCAAACAUAUCAUU) was designed to mimic endogenous mature miR-190 in PASMCs. One single stranded antisense oligonucleotides complementary to the mature miR-190 (Amo-190, ACCUAAUAUAUCAAACAUAUCA) was synthesized to specifically target and knockdown endogenous mature miR-190 in PASMCs. The end was locked by a methylene bridge between the 2′-O- and the 4′-C atoms to increase its stability. A scrambled RNA (scrambled RNA, sense: UUCUCCGAACGUGUCACGUTT; antisense: ACGUGACACGUUCGGAGAATT) was used as negative control of miR-190. The transfection efficiency was evaluated using 5′-Carboxyfluorescein (FAM)-labeled scrammed RNA (scrambled RNA-FAM). All the nucleic acids were synthesized by GenePharma Company (Shanghai, China).

### DUAL LUCIFERASE REPORTER GENE CONSTRUCTION

The constructions of dual luciferase reporters were performed as previous described [Li et al., 2013]. Briefly, a fragment of the *Kcnq5* mRNA (NM_001160130.1) (CAGGCATAGCAGTTCTTTAGCCATACATATCATTGCATGAACTATTTCGAAAGC) containing the predicted binding site for rno-miR-190 was synthesized and subcloned into the downstream of the *Renilla* luciferase reporter gene of the pGL3-promoter luciferase expression reporter vector (Invitrogen) named as pGL3-Kcnq5 3′-UTR reporter. A mutated fragment of the *Kcnq5* mRNA (CAGGCATAGCAGTTCTTTAGCCATACATAGTCTTGCATGAACTATTTCGAAAGC) was synthesized and sub-cloned into the downstream of the *Renilla* luciferase reporter gene of the pGL3-promoter luciferase expression reporter vector named as Mut pGL3-Kcnq5 3′-UTR reporter.

### SYNTHESIS OF miR-190 EXPRESSION VECTOR

The construction of miR-190 expression vector was performed by Invitrogen Life Tech. Briefly, the precursor dsDNA encoding mature rno-miR-190 was synthesized and subcloned into pcDNA™6.2-GW/EmGFPmiR expression vector named as pcDNA6.2-miR-190. pcDNA™6.2-GW/EmGFPmiR expression vector containing precursor dsDNA encoding a mature scrambled miRNA named as pcDNA6.2-scrambled miR.

### LUCIFERASE ASSAY

*Kcnq5* mRNA 3′-UTR/mutant of *Kcnq*5 mRNA 3′-UTR and scrambled miRNA/miR-190 were co-transfected into HEK293 cells. Luciferase

activities were measured using a dual luciferase reporter assay system (Promega) on a luminometer (Lumat LB9507) as previous described [Li et al., 2013]. Briefly, HEK293 cells were grown to 90% confluence in white 6-well plates in DMEM supplemented with 10% FBS at 37 °C under 5% $CO_2$. Cells were co-transfected with different constructs, which divided into four groups: (1) Kcnq5 3′-UTR + empty vector; (2) Kcnq5 3′-UTR + pcDNA6.2-scrambled miR; (3) Kcnq5 3′-UTR + pcDNA6.2-miR-190; (4) Mut Kcnq5 3′-UTR + pcDNA6.2-miR-190. For each group, a total of 25 ng of the thymidine kinase driven *Renilla* luciferase expression vector (pRL-TK) was transfected for normalization and as an internal control for transfection efficiency.

### WESTERN BLOT ASSAY

Proteins extracted from PASMCs and PAs were detected using a standard Western blot protocol. The antibody specific for β-actin was used as an internal control.

### STATISTICAL ANALYSIS

The composite data were expressed as mean ± SEM (standard error). Comparisons of data were accomplished by one-way ANOVA followed by Dunnett test or student's t-TEST. The differences between means were considered significantly different when $P < 0.05$.

## RESULTS

### miR-190 DISTRIBUTION AND EXPRESSION RESPONSE TO HYPOXIA

The rat model of PAH was produced by a consecutive hypoxic exposure for 9 days [Zhu et al., 2003]. Morphological changes of PAs were examined in tissues from the animals with H&E stain. Compared with the normoxic group, PA medial thickening was found in hypoxic rats, increasing by 33.5% ± 0.2 (n = 3 animals for each group) (Fig. 1A and 1B).

The location of miR-190 in PA was examined using *in situ* hybridization histochemistry. The miR-190 was mainly expressed in PASMCs. Consistently, our PCR analysis showed the miR-190 expression in the PA tissue. The real-time quantitative PCR (qPCR) analysis indicated that the miR-190 expression level was augmented by hypoxia in PAs (Fig. 1C–E).

### miR-190 AUGMENTED THE PE AND KCL INDUCED VASOCONSTRICTION OF ENDOTHELIUM-DENUDED PA RINGS

To test whether miR-190 has effects on vascular tone and constriction response of PAs to vasoconstrictors, the isolated endothelium-denuded PA rings from normoxic rats were transfected with synthetic miR-190 (miR-190) or co-transfected with synthetic miR-190 and Amo-190 (miR-190+Amo). The rings were tested with cumulative dose response curve to phenylephrine (PE) ($10^{-9}$ to

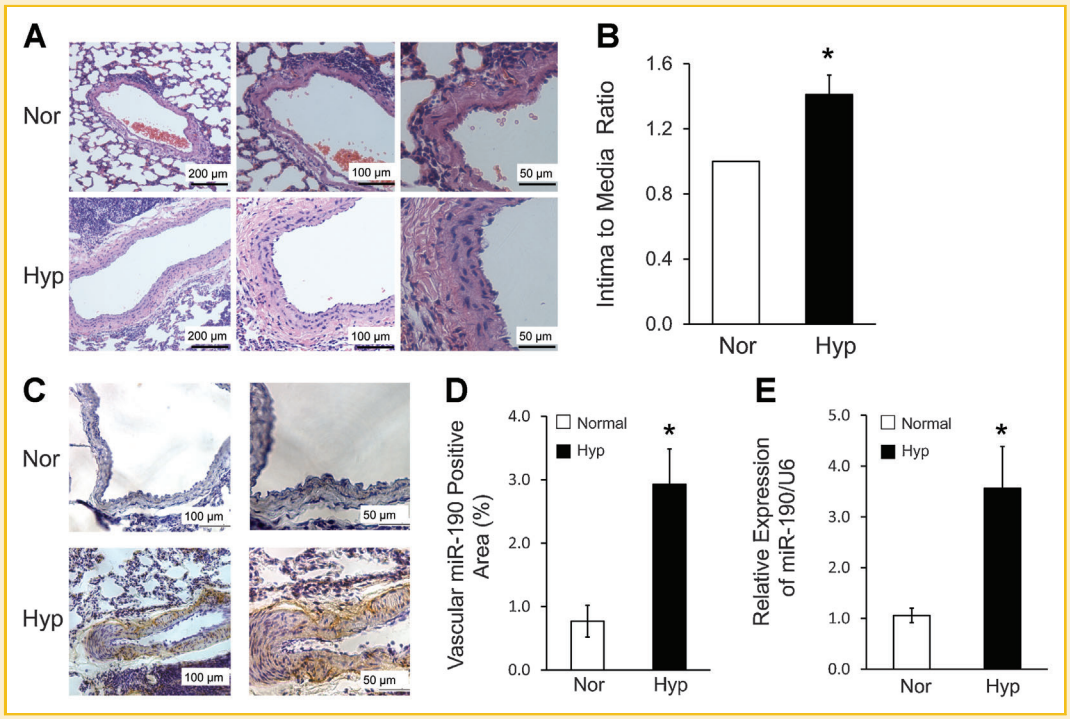


**Fig. 1.** Identification of hypoxia induced miR-190. A, characterization of hypoxic rat model. Sections of lung tissues from rats exposed to normoxic or hypoxic conditions were identified using H&E staining. Scale bars are 200, 100, and 50 μm. B, summarized data represented the ratios of intimal-to-medial areas of the vessel. C, localization of miR-190 by *in situ* hybridization in lung tissues from normoxic and hypoxic rats. Scale bars are 100, and 50 μm. D, quantitative analyses of positive staining per vascular area. E, qRT-PCR verification of the expression of miR-190 in PAs from normoxic and hypoxic rats. Nor, normoxic conditions; Hyp, hypoxic conditions; *$P < 0.05$. (A–D, n = 3 animals for each group; E, n = 3–6 separated experiments).

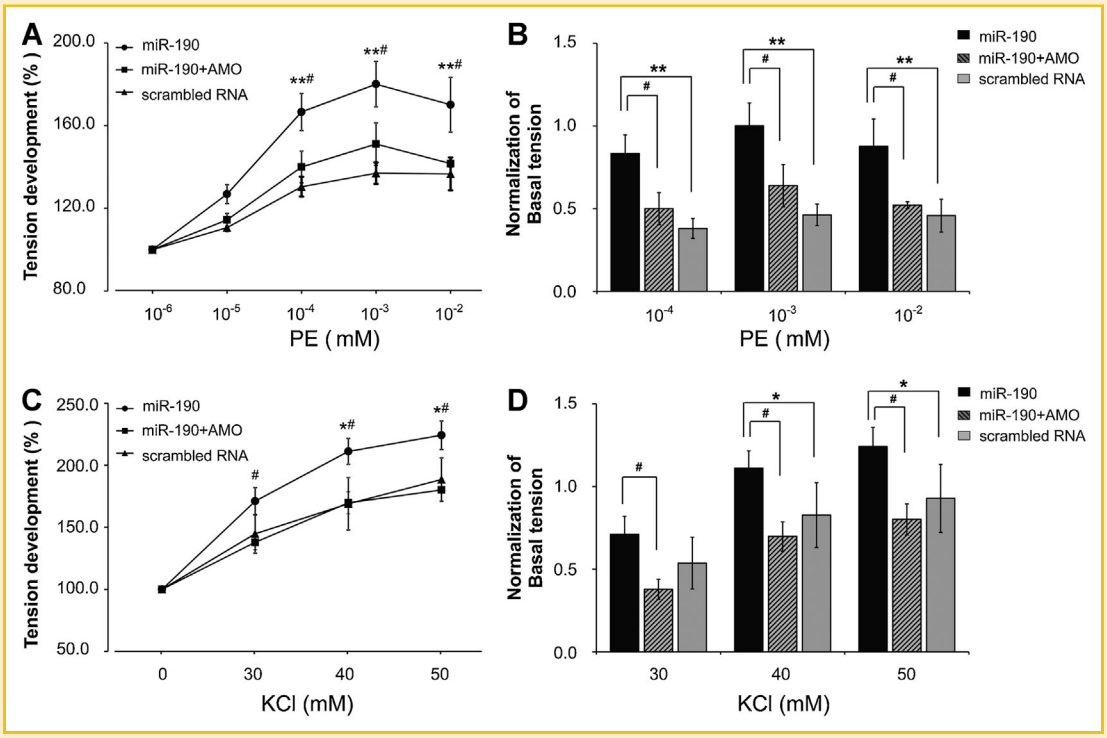


**Fig. 2.** The effect of miR-190 on pulmonary arterial tension. A and B, the endothelium-denuded PAs were transfected with different groups and preloaded with 0.3 g tension force in a tissue bath. The relationship of the vasoconstriction force with PE concentrations was studied in pulmonary arterial rings. Baseline tension was taken as 100%. The increased contractile responses to PE normalizing to baseline were represented by bar graph. C and D, same study of was performed with KCl in pulmonary arterial rings. Baseline tension was taken as 100%. The increased contractile responses to KCl normalizing to baseline were represented by bar graph. Scrambled RNA, scrambled RNA transfected groups; miR-190, synthetic miR-190 transfected groups; miR-190 + AMO, synthetic miR-190 and Amo-190 cotransfected groups. $^{**}P < 0.01$, $^{*}P < 0.05$, verus scrambled RNA, $^{\#}P < 0.05$, versus miR-190 + AMO. (n = 4–6 rings).

$10^{-5}$M) or KCl (30–50 mM) 48 h after transfection. In scrambled RNA transfected endothelium-denuded rings, $10^{-7}$ to $10^{-5}$ M PE caused significant increase in tension (by $119.8 \pm 7.8$, $127.0 \pm 9.4$ and $107.1 \pm 5.9$% of the basal level, respectively). By contrast, this PE produced vasoconstriction was enhanced greatly in miR-190 transfected groups (by $166.6 \pm 9.0$, $180.1 \pm 11.0$ and $170.1 \pm 13.2$% of the basal tension, respectively).

Similarly, the KCl-induced vasoconstriction was also augmented in the concentrations 40 and 50 mM ($169.0 \pm 21.1$, $188.5 \pm 17.4$ in scrambled RNA transfected groups and $211.2 \pm 10.4$, $224.2 \pm 11.5$% basal tension in miR-190 groups). Meanwhile, miR-190 + Amo co-transfection partially reversed the effect of miR-190 on vasoconstriction (Fig. 2), suggesting that up-regulation of miR-190 in PASMCs may result in the increased PA response to vasoconstrictors.

The transfection efficiency was further validated using 5′-carboxyfluorescein (FAM)-labeled scrambled oligonucleotides (scrambled RNA-FAM). As shown in Fig. 3A and B, more than 90% PASMCs were transfected with the FAM labeled fluorescence tracer. The qPCR also showed the relative expression of miR-190 in different groups. miR-190 transfection led to $7.56 \pm 0.67$ times higher expression of miR-190 than that in scrambled RNA transfected groups. Co-transfection with Amo-190 efficiently reduced this enhancement to $2.35 \pm 0.19$ (Fig. 3C).

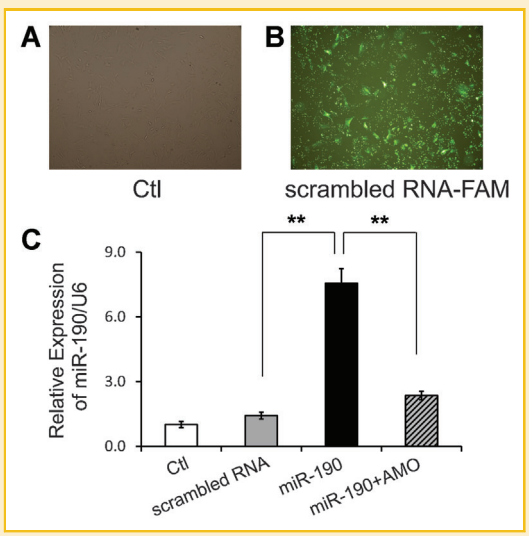


**Fig. 3.** Relative expression of miR-190 in PASMCs transfected with different groups. A, PASMCs cultured in normoxic conditions served as control. B, representative fluorescent images of scrambled RNA-FAM transfected groups. C, qRT-PCR verification of the expression of miR-190 in different transfected groups. Ctl, control; scrambled RNA -FAM, FAM labeled scrambled RNA; scrambled RNA, scrambled RNA transfected groups; miR-190, synthetic miR-190 transfected groups; miR-190 + AMO, synthetic miR-190 and Amo-190 cotransfected groups; $^{**}P < 0.01$. (n = 3 separated experiments).

### miR-190 RAISED INTRACELLULAR $Ca^{2+}$ IN PASMCS

As the elevation of $[Ca^{2+}]_i$ in PASMCs plays an important role in PVC, we studied the effect of miR-190 on $[Ca^{2+}]_i$ in PASMCs using the $Ca^{2+}$ imaging technique. As shown in Fig. 4A, KCl caused a transient and significant increase in $[Ca^{2+}]_i$ as indicated by the $FI/FI_0$ ratio in the control groups (Ctl) peaked at $1.80 \pm 0.02$ ($n = 18$ cells in three experiments). In PASMCs transfected with scrambled RNA groups, the KCl produced an increase in $[Ca^{2+}]_i$ to almost the same level, i.e., $1.85 \pm 0.02$ ($n = 21$ cells in three experiments, Fig. 4B). However, in linopirdine pretreated PASMCs, the KCl-induced increase in $[Ca^{2+}]_i$ was greater than that in Ctl and scrambled RNA groups, which was peaked at $2.27 \pm 0.09$ ($n = 9$ cells in three experiments, Fig. 4C). Similarly, in miR-190 transfected PASMCs, the KCl-induced increase in $[Ca^{2+}]_i$ was much greater than that in scrambled RNA groups, which was peaked at $2.54 \pm 0.09$ ($n = 26$ cells in three experiments, Fig. 4D). This effect was markedly diminished by a co-transfection of the miR-190 with Amo-190, as the $[Ca^{2+}]_i$ reached only $1.95 \pm 0.07$ ($n = 18$ cells in three experiments, Fig. 4E). All these changes were statistically significant (Fig. 4F, $P < 0.01$ or $P < 0.05$). With the analysis of area under the curve (AUC), we confirmed that with high $K^+$ induction, miR-190 transfection produced the similar increase in $[Ca^{2+}]_i$ with that produced by linopirdine. Meanwhile, Amo-190 co-transfection partially reversed the miR-190 induced $[Ca^{2+}]_i$ elevation, suggesting miR-190 may play a role in HPV by regulating intracellular $Ca^{2+}$ (Fig. 4G).

### VERIFICATION OF INTERACTIONS BETWEEN miR-190 AND ITS TARGET GENE

To test whether miR-190 directly targeted the 3′-UTR of *Kcnq*5 mRNA (Fig. 5A), we constructed luciferase reporter containing the predicted positive target sequence of miR-190 and its negative mutation (Fig. 5B and C). The luciferase assays showed that transient transfection of HEK293 cells with *Kcnq*5 mRNA 3′-UTR and miR-190 resulted in down-regulation of luciferase activity compared with scrambled miRNA co-transfected cells, which was eliminated when the predicted miR-190 binding site was mutated (Fig. 6A). All these changes were statistically significant ($P < 0.01$).

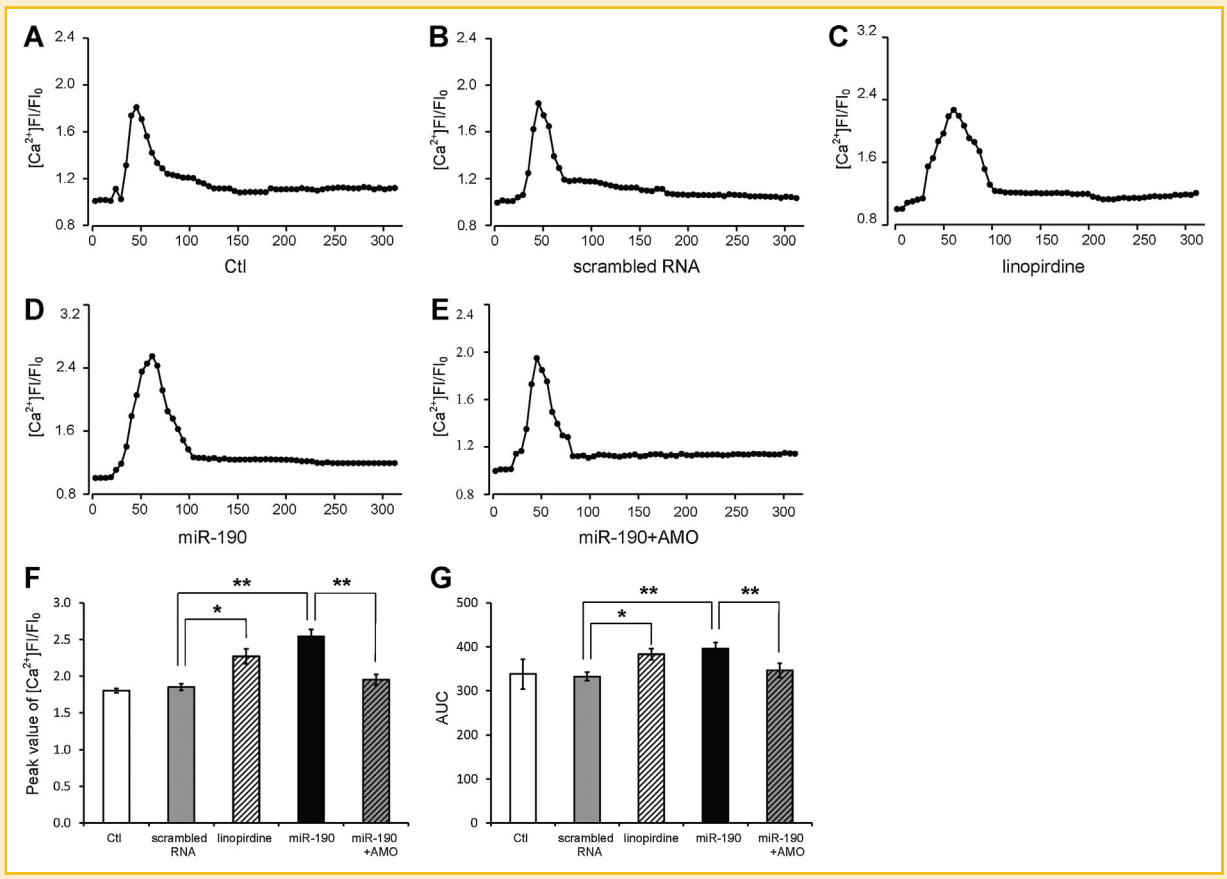


Fig. 4. The effect of miR-190 on $Ca^{2+}$ influx induced by KCl in PASMCs. The $[Ca^{2+}]_i$ FI was detected and recorded for 300 s at 5 s intervals. Cells were exposed to 120 mM KCl to trigger extracellular $Ca^{2+}$ entry after 20 s recording. A, Ctl ($n = 18$ cells in 3 experiments). B, scrambled RNA ($n = 21$ cells in 3 experiments). C, linopirdine ($n = 9$ cells in 3 experiments). D, miR-190 ($n = 26$ cells in 3 experiments). E, miR-190 + AMO ($n = 18$ cells in 3 experiments). F, the peak value ($[Ca^{2+}]_i$ $FI/FI_0$) of $Ca^{2+}$ response induced by KCl. G, the AUC of the $Ca^{2+}$ response induced by KCl. $^{**}P < 0.01$, $^{*}P < 0.05$. PASMCs, pulmonary arterial smooth muscle cells; FI, fluorescence intensity; $FI_0$, initial FI; $FI/FI_0$, FI normalizing to initial FI; Ctl, PASMCs without transfection served as control; scrambled RNA, scrambled RNA transfected groups; miR-190, synthetic miR-190 transfected groups; miR-190 + AMO, synthetic miR-190 and Amo-190 cotransfected groups; AUC, area under the curve; T (s), Time (seconds).

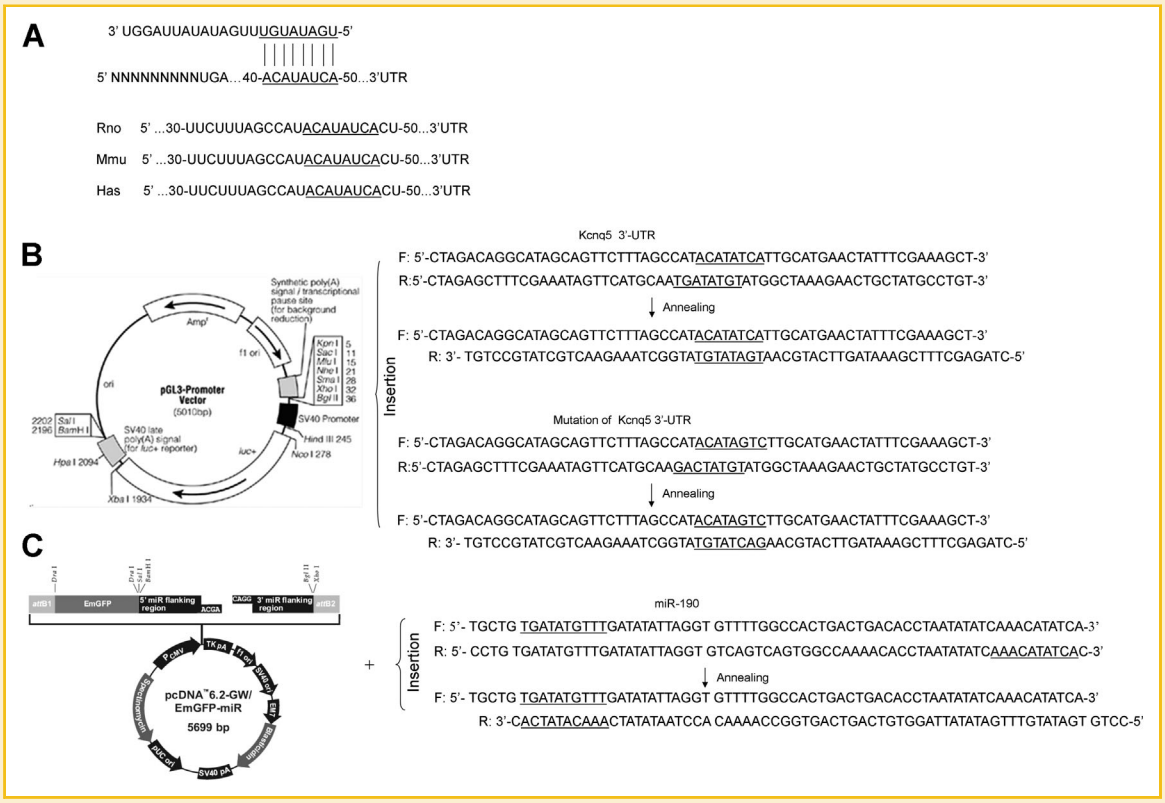


**Fig. 5.** Construction of expression vectors. A, computational analysis was performed for the complementarities of miR-190 seed sequence to the 3′-UTR of *Kcnq5* mRNA and conservation of the putative binding site in rat, human, and mouse. B, construction of pGL3-promoter luciferase expression reporter vector. A fragment of the *Kcnq5* mRNA containing the predicted binding site for rno- miR-190 was sub-cloned into the downstream of the *Renilla* luciferase reporter to create the construct named as *Kcnq5* 3′-UTR. Meanwhile, within the binding site, 3 sites were mutated and sub-cloned into the same reporter to form a mutated version of the Kcnq5 3′-UTR. C, schematic illustration of construction of pcDNA™6.2-GW/EmGFPmiR expression vector carrying miR-190. The precursor DNA encoding miR-190 was inserted into pcDNA™6.2-GW/EmGFPmiR expression vector named as pcDNA6.2-miR-190.

Subsequently, we studied the regulation of *Kcnq5* gene expression by miR-190. Western blot analysis showed the expression of Kcnq5 (Kv7.5) in PAs obtained from normoxic and hypoxic rats. The Kv7.5 protein expression level was greatly reduced when the up-regulation of miR-190 occurred under hypoxic conditions ($P < 0.05$, Fig. 6B). There was an inverse correlation between miR-190 and Kv7.5 expression. The expression of Kv7.5 in the protein level was greatly suppressed in the miR-190-transfected PASMCs compared with scrambled RNA transfected groups, and this reduction was efficiently reversed by co-transfection with Amo-190 (Fig. 6C), suggesting that *Kcnq5* mRNA seemed to be the target for miR-190.

## DISCUSSION

In this study, we found that miR-190 was up-regulated in PASMCs by hypoxic exposure. Overexpression of miR-190 affected PA vasoconstriction by increasing the $Ca^{2+}$ influx, and one candidate target of miR-190, *Kcnq5* mRNA, was implicated.

Several recent studies have shown the importance role of miRs in pathological process of cardiovascular diseases [Kwon et al., 2005; Divakaran and Mann, 2008; Thum et al., 2008]. Also, miRs have been proved to be involved in regulating PAH by regulating gene expression and signaling pathways. For example, hypoxia induced up-regulation of miR-21 has been shown to play a significant role in hypoxia-induced cell fates by regulating multiple gene targets [Bao et al., 2012; Zhang et al., 2012]. The abnormal expression of miR-204, in both human and rodent PAH, are shown to regulate multiple target gene expression and signaling pathways (Src/stat3 cascade, NFAT activation, BMPR2 down-regulation, IL-6 production), affecting PASMC proliferation and apoptosis in the pathophysiological processes in PAH. In vitro studies further proved the role of miR-204 in reversing symptoms of PAH in the rat model, providing a novel therapeutic approach for human PAH [Courboulin et al., 2011; Paulin et al., 2011]. MiR-24 has also been implicated in the PDGF and TGF-β pathways to control the VSMC phenotype indicating an important role of miRNAs in differentiation of VSMCs [Chan et al., 2010]. Moreover, in our previous studies, we have proved that hypoxia-induced up-regulation of miR-138 in PAs suppresses the apoptosis of PASMCs contributing to the pathogenesis of HPVR by repression of Mst1 and its downstream signaling: Akt signaling [Li et al., 2013]. Meanwhile, overexpression of miR-328 in the transgenic mice remarkably decreases the right ventricular systolic

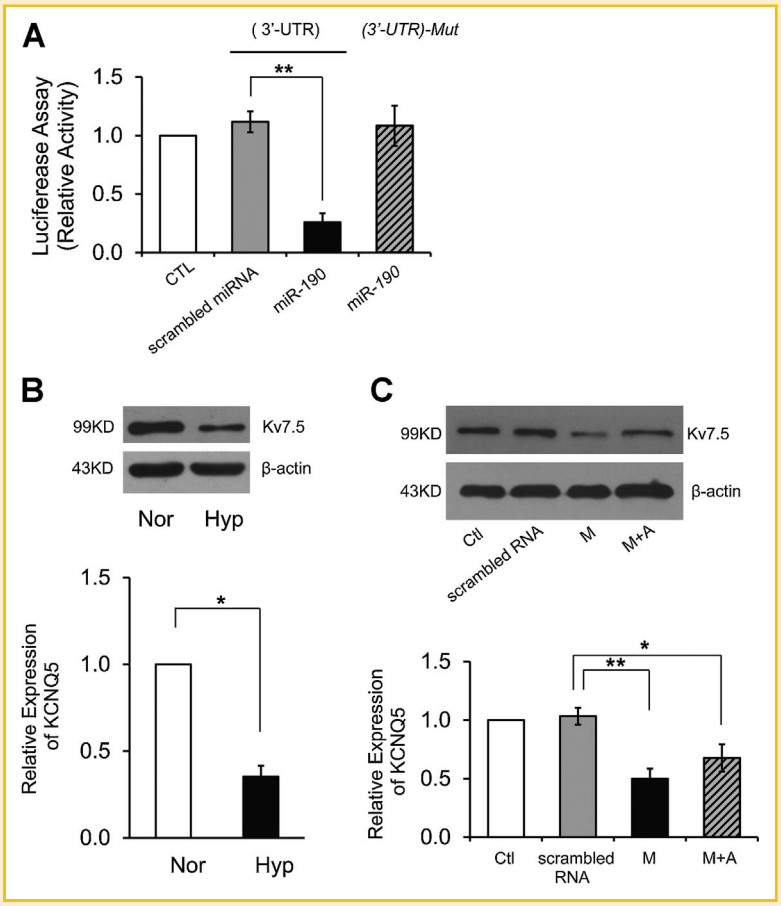


**Fig. 6.** The effect of miR-190 on *Kcnq5* mRNA. A, luciferase assay in HEK293 cells for the posttranscriptional repression of *Kcnq5* mRNA. HEK293 cells co-transfected with *Kcnq5* 3′-UTR and empty vector was served as control (CTL); HEK293 cells were co-transfected with *Kcnq5* 3′-UTR and scrambled miRNA, miR-190 and *Kcnq5* 3′-UTR, and miR-190 and mutant *Kcnq5* 3′-UTR, respectively. B, the expression pattern of Kv7.5 in the PAs isolated from normoxic and hypoxic rats. C, Western blot assay in PASMCs transfected with different groups. The expression of Kv7.5 was normalized to β-actin and represented by the bar graph. PASMCs without any transfection served as control (Ctl); scrambled RNA, scrambled RNA transfected groups; M, synthetic miR-190 transfected groups; M + A, synthetic miR-190 and Amo-190 cotransfected groups; *Kcnq5*, The voltage-gated $K^+$ channel subfamily member 5; Kv7.5, *Kcnq5* encoded product; 3′-UTR, 3′-UTR of *Kcnq5* mRNA; Mut, mutant; Nor, normoxia; Hyp, hypoxia. $^*P < 0.05$, $^{**}P < 0.01$. (n = 3–6 separated experiments).

pressure and pulmonary artery wall thickness under both normoxic and hypoxic conditions, implicating an important protecting role for miR-328 in hypoxic pulmonary artery constriction [Guo et al., 2012]. All these studies suggest the importance of microRNAs (miRNAs) in vascular tones and cell fates and the consequential effects on PH.

According to bioinformatics-based analysis, *Kcnq5* mRNA has been identified to be a direct target for miR-190 involved in HPV. The functional role for Kcnq channel in regulating voltage-dependent $Ca^{2+}$ influx and contraction in pulmonary artery smooth muscle cells has been implicated in recent studies [Ohya et al., 2003; Mani et al., 2009]. Thus, in the present study, we had been focused on miR-190 and shown its effect on the PA vasoconstriction. The underlying mechanism was also studied.

We used miR-190 synthetic mimics and its anti-oligonucleotides to manipulate the expression of miR-190 in PASMCs. Consistent with our hypothesis, synthetic miR-190 could enhance PE and KCl-induced PA vasoconstriction, indicating the role of hypoxic augment of miR-190 in HPV. We further detected the $Ca^{2+}$ influx in cultured PASMCs. We used high concentration of $K^+$ to produce depolarization, which can lead to the subsequent extracellular $Ca^{2+}$ entry. In PASMCs pretreated with linopirdine, KCl triggered $Ca^{2+}$ influx was enhanced, indicating more depolarization was produced by blocking Kv7 activity. As the SMC membranes are not only permeable to $K^+$ but also to other ions (like sodium and chloride ions) to certain degree. By suppressing the activity of Kv7, the contributions of other ions including $Na^+$ and $Ca^{2+}$ to the reversal membrane potential may emerge. Thus, linopirdine still can produce more depolarization. Similarly, in miR-190 transfected cells, the $Ca^{2+}$ influx was also enhanced, suggesting that miR-190 may enhance the L-type $Ca^{2+}$ channel dependent $Ca^{2+}$ entry in smooth muscles cells by regulating Kv7 channel activity. And the miR-190 induced PA dysfunction was at least caused by the increased $[Ca^{2+}]_i$. Although electrophysiological measurement was lacking, data from $Ca^{2+}$ imaging still implied a link between miR-190 and Kv7 channel activity. Moreover, in molecular studies, hypoxia can decrease the

expression of Kv7.5, the subfamily member of voltage-gated $K^+$ channel, indicating one target mRNA for miR-190 regulating. Consistent with bioinformatics-based analysis, luciferase reporter and Western blot assays further validated *Kcnq5* mRNA to be a direct target for miR-190 at the post-transcriptional level. Obviously, how loss of Kv7 channel activity to modify the level of depolarization and whether the miR-190 regulated PA constriction is directly by targeting *Kcnq5* mRNA, are still need to be further confirmed. More than one mechanism maybe involved in miR-190 regulated vasoconstriction. The rescue effects of restoring Kv7.5 expression on $Ca^{2+}$ influx and enhanced vasoconstriction would be justified in the further studies. Still, all strong evidences indicated the role for miR-190 in regulating PA constriction. One target mRNA for miR-190, *Kcnq5* mRNA, was also proved.

Recent studies have shown that miR-190 contributes to arsenic-induced Akt activation in carcinogenicity by suppressing PH domain leucine-rich repeat protein phosphatase (PHLPP) [Beezhold et al., 2011]. The up-regulation of miR-190 is frequently associated with a variety of cancers, including breast cancer, pancreatic tumor cells and dormant tumors [Almog et al., 2013; Lowery et al., 2009; Zhang et al., 2009]. Thus, the regulation of the expression of miR-190 may be a potential tumor regulator in different carcinomas. Herein, our data firstly illustrate the role of miR-190 augment in PASMCs constitute a significant step toward the understanding of the molecular mechanisms of HPV in hypoxic PAH.

Obviously, other unidentified miR-190 targets may contribute to the pathological process of HPV. The involvement of other potential targets also should be studied in the future. Nevertheless, the aberrant expression of the global miRNAs in hypoxic PAH suggests that post-transcriptional gene regulation by miRNAs is an important step in hypoxic PAH pathogenesis. However, possible mechanisms that control the expression of miRNAs in hypoxic PAH are still unclear and understanding of that in PH is vital for designing novel therapeutic strategy.

In conclusion, our studies provide new evidence showing that miR-190 plays an important role in the vascular constriction. Under hypoxic condition, the enhanced effect of miR-190 may be attribute to a repression of *Kcnq5* mRNA expression, which, in turn, results in the elevation of $[Ca^{2+}]_i$ in PASMCs and abnormal PA constriction. Therefore, the stabilization of the miR-190 level may be a novel strategy for clinical treatment of hypoxic PAH in the future.

## ACKNOWLEGMENTS

We thank Dr. Chun Jiang at Georgia State University, USA for his comments on this manuscript.

## REFERENCES

Almog N, Briggs C, Beheshti A, Ma L, Wilkie KP, Rietman E, Hlatky L. 2013. Transcriptional changes induced by the tumor dormancy-associated micro-RNA-190. Transcription 4.

Archer S, Rich S. 2000. Primary pulmonary hypertension: a vascular biology and translational research "Work in progress". Circulation 102: 2781–2791.

Bao B, Ahmad A, Kong D, Ali S, Azmi AS, Li Y, Banerjee S, Padhye S, Sarkar FH. 2012. Hypoxia induced aggressiveness of prostate cancer cells is linked with deregulated expression of VEGF, IL-6 and miRNAs that are attenuated by CDF. PloS One 7:e43726.

Beezhold K, Liu J, Kan H, Meighan T, Castranova V, Shi X, Chen F. 2011. MiR-190-mediated downregulation of PHLPP contributes to arsenic-induced Akt activation and carcinogenesis. Toxicol Sci 123:411–420.

Caruso P, Dempsie Y, Stevens HC, McDonald RA, Long L, Lu R, White K, Mair KM, McClure JD, Southwood M, Upton P, Xin M, van Rooij E, Olson EN, Morrell NW, MacLean MR, Baker AH. 2012. A role for miR-145 in pulmonary arterial hypertension: evidence from mouse models and patient samples. Circ Res 111:290–300.

Chan MC, Hilyard AC, Wu C, Davis BN, Hill NS, Lal A, Lieberman J, Lagna G, Hata A. 2010. Molecular basis for antagonism between PDGF and the TGFbeta family of signalling pathways by control of miR-24 expression. The EMBO J 29:559–573.

Charlton SJ, Vauquelin G. 2010. Elusive equilibrium: the challenge of interpreting receptor pharmacology using calcium assays. Br J Pharmacol 161:1250–1265.

Chin KM, Rubin LJ. 2008. Pulmonary arterial hypertension. J Am Coll Cardiol 51:1527–1538.

Courboulin A, Paulin R, Giguere NJ, Saksouk N, Perreault T, Meloche J, Paquet ER, Biardel S, Provencher S, Cote J, Simard MJ, Bonnet S. 2011. Role for miR-204 in human pulmonary arterial hypertension. J Exp Med 208: 535–548.

Delmas P, Brown DA. 2005. Pathways modulating neural KCNQ/M (Kv7) potassium channels. Nat Rev Neurosci 6:850–862.

Divakaran V, Mann DL. 2008. The emerging role of microRNAs in cardiac remodeling and heart failure. Circ Res 103:1072–1083.

Eddahibi S, Morrell N, d'Ortho MP, Naeije R, Adnot S. 2002. Pathobiology of pulmonary arterial hypertension. Eur Respir J 20:1559–1572.

Grant JS, White K, Maclean MR, Baker AH. 2013. MicroRNAs in pulmonary arterial remodeling. Cell Mol Life Sci 70(23):4479–4494.

Guazzi MD, Alimento M, Berti M, Fiorentini C, Galli C, Tamborini G. 1989. Enhanced hypoxic pulmonary vasoconstriction in hypertension. Circulation 79:337–343.

Guo L, Qiu Z, Wei L, Yu X, Gao X, Jiang S, Tian H, Jiang C, Zhu D. 2012. The microRNA-328 regulates hypoxic pulmonary hypertension by targeting at insulin growth factor 1 receptor and L-type calcium channel-alpha1C. Hypertension 59:1006–1013.

Humbert M, Morrell NW, Archer SL, Stenmark KR, MacLean MR, Lang IM, Christman BW, Weir EK, Eickelberg O, Voelkel NF, Rabinovitch M. 2004. Cellular and molecular pathobiology of pulmonary arterial hypertension. J Am Coll Cardiol 43:13S–24S.

Ikeda S, Kong SW, Lu J, Bisping E, Zhang H, Allen PD, Golub TR, Pieske B, Pu WT. 2007. Altered microRNA expression in human heart disease. Physiol Genomics 31:367–373.

Joshi S, Balan P, Gurney AM. 2006. Pulmonary vasoconstrictor action of KCNQ potassium channel blockers. Respir Res 7:31.

Kumar MS, Lu J, Mercer KL, Golub TR, Jacks T. 2007. Impaired microRNA processing enhances cellular transformation and tumorigenesis. Nat Genet 39:673–677.

Kwon C, Han Z, Olson EN, Srivastava D. 2005. MicroRNA1 influences cardiac differentiation in Drosophila and regulates Notch signaling. Proc Natl Acad Sci USA 102:18986–18991.

Li S, Ran Y, Zhang D, Chen J, Zhu D. 2013. MicroRNA-138 plays a role in hypoxic pulmonary vascular remodelling by targeting Mst1. Biochem J 452:281–291.

Li S, Ran Y, Zheng X, Pang X, Wang Z, Zhang R, Zhu D. 2010. 15-HETE mediates sub-acute hypoxia-induced TRPC1 expression and enhanced

capacitative calcium entry in rat distal pulmonary arterial myocytes. Prostaglandins Other Lipid Mediat 93:60–74.

Lowery AJ, Miller N, Devaney A, McNeill RE, Davoren PA, Lemetre C, Benes V, Schmidt S, Blake J, Ball G, Kerin MJ. 2009. MicroRNA signatures predict oestrogen receptor, progesterone receptor and HER2/neu receptor status in breast cancer. Breast cancer research. Breast Cancer Res 11:R27.

Mackie AR, Brueggemann LI, Henderson KK, Shiels AJ, Cribbs LL, Scrogin KE, Byron KL. 2008. Vascular KCNQ potassium channels as novel targets for the control of mesenteric artery constriction by vasopressin, based on studies in single cells, pressurized arteries, and in vivo measurements of mesenteric vascular resistance. J Pharmacol Exp Ther 325:475–483.

Mackie AR, Byron KL. 2008. Cardiovascular KCNQ (Kv7) potassium channels: physiological regulators and new targets for therapeutic intervention. Mol Pharmacol 74:1171–1179.

Mani BK, Brueggemann LI, Cribbs LL, Byron KL. 2009. Opposite regulation of KCNQ5 and TRPC6 channels contributes to vasopressin-stimulated calcium spiking responses in A7r5 vascular smooth muscle cells. Cell Calcium 45:400–411.

Mauban JR, Remillard CV, Yuan JX. 2005. Hypoxic pulmonary vasoconstriction: role of ion channels. J Appl Physiol 98:415–420.

Moudgil R, Michelakis ED, Archer SL. 2005. Hypoxic pulmonary vasoconstriction. J Appl Physiol 98:390–403.

Ohya S, Sergeant GP, Greenwood IA, Horowitz B. 2003. Molecular variants of KCNQ channels expressed in murine portal vein myocytes: a role in delayed rectifier current. Circ Res 92:1016–1023.

Ono K, Kuwabara Y, Han J. 2011. MicroRNAs and cardiovascular diseases. FEBS J 278:1619–1633.

Oparil S, Zaman MA, Calhoun DA. 2003. Pathogenesis of hypertension. Ann Intern Med 139:761–776.

Paulin R, Meloche J, Jacob MH, Bisserier M, Courboulin A, Bonnet S. 2011. Dehydroepiandrosterone inhibits the Src/STAT3 constitutive activation in pulmonary arterial hypertension. Am J physiol Heart Circ Physiol 301: H1798–H1809.

Remillard CV, Yuan JX. 2005. High altitude pulmonary hypertension: role of K+ and Ca2+ channels. High Alt Med Biol 6:133–146.

Robbins J. 2001. KCNQ potassium channels: physiology, pathophysiology, and pharmacology. Pharmacol Ther 90:1–19.

Sandoval Zarate J. 2006. Pulmonary arterial hypertension. Arch Cardiol Mex 76(Suppl 2):S69–S75.

Sweeney M, Yuan JX. 2000. Hypoxic pulmonary vasoconstriction: role of voltage-gated potassium channels. Respir Res 1:40–48.

Thum T, Gross C, Fiedler J, Fischer T, Kissler S, Bussen M, Galuppo P, Just S, Rottbauer W, Frantz S, Castoldi M, Soutschek J, Koteliansky V, Rosenwald A, Basson MA, Licht JD, Pena JT, Rouhanifard SH, Muckenthaler MU, Tuschl T, Martin GR, Bauersachs J, Engelhardt S. 2008. MicroRNA-21 contributes to myocardial disease by stimulating MAP kinase signalling in fibroblasts. Nature 456:980–984.

Voelkel NF, Gomez-Arroyo J, Abbate A, Bogaard HJ, Nicolls MR. 2012. Pathobiology of pulmonary arterial hypertension and right ventricular failure. Eur Respir J 40:1555–1565.

Weir EK, Cabrera JA, Mahapatra S, Peterson DA, Hong Z. 2010. The role of ion channels in hypoxic pulmonary vasoconstriction. Adv Exp Med Biol 661: 3–14.

Yeung SY, Greenwood IA. 2005. Electrophysiological and functional effects of the KCNQ channel blocker XE991 on murine portal vein smooth muscle cells. Br J Pharmacol 146:585–595.

Yeung SY, Pucovsky V, Moffatt JD, Saldanha L, Schwake M, Ohya S, Greenwood IA. 2007. Molecular expression and pharmacological identification of a role for K(v)7 channels in murine vascular reactivity. Br J Pharmacol 151:758–770.

Zavisca FG, Stanley TH, Cronau LH, Iacono C. 1993. A new model to evaluate the hypertensive response to noxious stimuli in the anesthetized, spontaneously hypertensive rat. Anesth Analg 77:788–794.

Zhang L, Dong LY, Li YJ, Hong Z, Wei WS. 2012. MiR-21 represses FasL in microglia and protects against microglia-mediated neuronal cell death following hypoxia/ischemia. Glia 60:1888–1895.

Zhang W, Dahlberg JE, Tam W. 2007. MicroRNAs in tumorigenesis: a primer. Am J Pathol 171:728–738.

Zhang Y, Li M, Wang H, Fisher WE, Lin PH, Yao Q, Chen C. 2009. Profiling of 95 microRNAs in pancreatic cancer cell lines and surgical specimens by real-time PCR analysis. World J Surg 33:698–709.

Zheng X, Li Q, Tang X, Liang S, Chen L, Zhang S, Wang Z, Guo L, Zhang R, Zhu D. 2008. Source of the elevation Ca2+ evoked by 15-HETE in pulmonary arterial myocytes. Eur J Pharmacol 601:16–22.

Zhong XZ, Harhun MI, Olesen SP, Ohya S, Moffatt JD, Cole WC, Greenwood IA. 2010. Participation of KCNQ (Kv7) potassium channels in myogenic control of cerebral arterial diameter. J physiology 588:3277–3293.

Zhu D, Medhora M, Campbell WB, Spitzbarth N, Baker JE, Jacobs ER. 2003. Chronic hypoxia activates lung 15-lipoxygenase, which catalyzes production of 15-HETE and enhances constriction in neonatal rabbit pulmonary arteries. Circ Res 92:992–1000.